Nanoscale Advances

ROYAL SOCIETY OF CHEMISTRY

COMMUNICATION

View Article Online
View Journal | View Issue

Cite this: *Nanoscale Adv.*, 2024, **6**, 4360

Received 16th May 2024
Accepted 6th July 2024

DOI: 10.1039/d4na00414k

rsc.li/nanoscale-advances

Magnetically recoverable Fe_3O_4@SiO_2@SBA-3@2-ATP-Cu: an improved catalyst for the synthesis of 5-substituted 1*H*-tetrazoles†

Zahra Heidarnezhad,[a] Arash Ghorbani-Choghamarani *[b] and Zahra Taherinia [a]

Functionalization of Fe_3O_4@SiO_2@SBA-3 with double-charged 3-chloropropyltrimethoxysilane (CPTMS) and 2-aminophenol, followed by mechanical mixing of the solid product with copper(I) chloride produces a new, greener and efficient Fe_3O_4@SiO_2@SBA-3@2-ATP-Cu catalyst for the synthesis of 5-substituted 1*H*-tetrazoles. XRD, SEM, atomic absorption, TGA, N_2 adsorption–desorption, and VSM analyses were performed for the characterization of the Fe_3O_4@SiO_2@SBA-3@2-ATP-Cu structure. Nitrogen adsorption–desorption analysis revealed that Fe_3O_4@SiO_2@SBA-3@2-ATP-Cu has a surface area of 242 m^2 g^{-1} and a total pore volume of 55.72 cm^3 g^{-1}. In synthesizing 5-substituted 1*H*-tetrazoles, Fe_3O_4@SiO_2@SBA-3@2-ATP-Cu shows superior yields in short reaction times at 120 °C. This catalyst also showed high thermal stability and recyclability at least for 4 runs without apparent loss of efficiency.

Introduction

For decades, researchers have widely searched for ways to synthesize porous materials with high surface area and very diverse contents.[1–5] Among these porous solid compounds, mesoporous materials such as MCM-41, MCM-48, SBA-15, and SBA-3 have attracted more attention than others due to their applications in many areas.[6–10] The main differences in the preparation of mesoporous materials are the type of used templates (ionic surfactant for MCM-41 and triblock copolymer in the case of SBA-15) and the synthesis medium (MCM-41 prepared in the basic medium, and SBA-15 prepared in the acidic medium).[11] SBA-type materials (SBA-15, SBA-3) show much higher stability than MCM-41 due to the contribution of some micropores connecting mesopores.[12] However, the chemical inertness of SBA-15, which is mainly composed of silicon dioxide, greatly limits its application in chemical engineering, especially in heterogeneous catalysis. Incorporated heteroatoms are commonly used to form active sites in the mesoporous silica framework and confer acid sites and catalytic activities to the silica matrix.[13–15] In the literature, applications of SBA-3 as a catalyst support are rarely reported.[16–20] The use of magnetic nanoparticles provides both economic and ecological benefits due to their properties, low toxicity, and simple separation by an external magnetic field.[21–23] Magnetic nanoparticles have been widely employed as novel magnetically recoverable catalysts in medicinal applications,[24–26] drug delivery,[27,28] and industry.[29,30]

On the other hand, tetrazoles are a valuable class of heterocycles, which have been recently used as both anticancer[31,32] and antimicrobial agents.[33,34] They have received increased attention due to their potential biological activities,[35–37] and industrial applications.[38–40] A versatile method for the preparation of tetrazole is based on [3 + 2] cycloaddition of the azide ion and organic nitriles in the presence of a catalyst.[41–47] Although the reported methods are effective, they are limited due to the use of toxic solvents, tedious workup, difficulty in separation, and expensive catalysts. As part of our continuous efforts into the design of modified magnetic mesoporous silica nanoparticles and their application in organic synthesis,[48,49] we report here the preparation of Fe_3O_4@SiO_2@SBA-3@2-ATP-Cu (Scheme 1), and its performance for the synthesis of 5- substituted 1*H*-tetrazoles.

Experimental

Preparation of Fe_3O_4@SiO_2@SBA-3@2-ATP-Cu

Fe_3O_4@SiO_2@SBA-3 was readily synthesized similar to a previously reported study.[48] Briefly, the catalyst was prepared by adding 1.5 mL of (3-chloropropyl)triethoxysilane (CPTES) to a suspension of Fe_3O_4@SiO_2@SBA-3 (1 g)

[a]*Department of Chemistry, Faculty of Science, Ilam University, Ilam, Iran*
[b]*Department of Organic Chemistry, Faculty of Chemistry and Petroleum Sciences, Bu-Ali Sina University, Hamedan 6517838683, Iran. E-mail: a.ghorbani@basu.ac.ir; arashghch58@yahoo.com; Fax: +988138380709; Tel: +988138282807*

† Electronic supplementary information (ESI) available. See DOI: https://doi.org/10.1039/d4na00414k

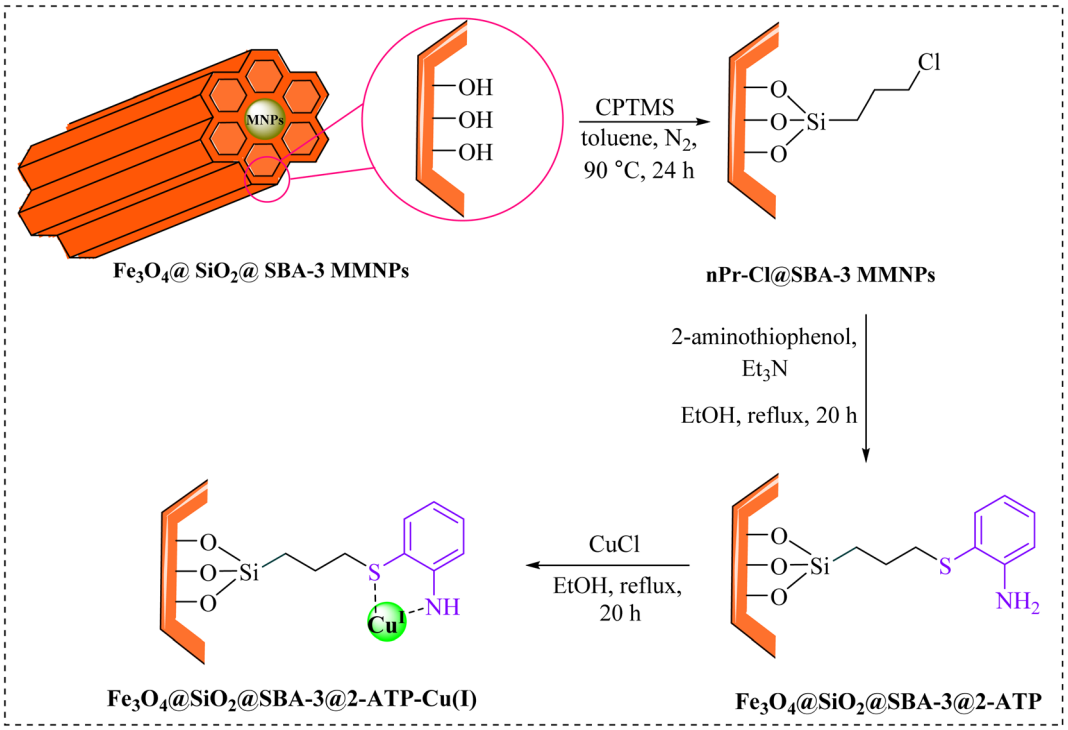

Scheme 1 Preparation of Fe_3O_4@SiO_2@SBA-3@2-ATP-Cu.

in 25 mL of toluene, followed by mechanical mixing of the solid product at 90 °C for 24 h. The Fe_3O_4@SiO_2@SBA-3@CPTMS material (1 g) was then treated with 2-aminothiophenol (1.5 g) and trimethylamine (3 mL), followed by subsequent thermal treatment of the reaction mixture at 78 °C in ethanol for 20 h, affording Fe_3O_4@SiO_2@SBA-3@CPTMS@ATP, and then the resulting material was then washed with ethanol, and dried at room temperature. Finally, Fe_3O_4@SiO_2@SBA-3@CPTMS@ATP (1 g) in 25 mL of ethanol was sonicated for 10 min. Then, the resulting nanoparticles (Fe_3O_4@SiO_2@SBA-3@CPTMS@ATP) were filtered, washed with ethanol (70% v/v), and dried at room temperature. The obtained Fe_3O_4@SiO_2@SBA-3@CPTMS@ATP (0.5 g) was dispersed in 25 mL of ethanol and was sonicated for 10 min, and then copper(I) chloride (2 mmol) was added to the reaction mixture. The reaction mixture was stirred at 80 °C for 24 h. After the separation of the final product by an external magnet, Fe_3O_4@SiO_2@SBA-3@2-ATP-Cu was washed with ethanol and consequently dried in an oven at 55 °C.

General procedure for the synthesis of 5-substituted 1*H*-tetrazoles

A sealed tube was charged with nitrile (1 mmol), sodium azide (1.1 mmol), and Fe_3O_4@SiO_2@SBA-3@2-ATP-Cu (60 mg) at 120 °C, and then polyethylene glycol (1 mL) was added. The resulting mixture was stirred under reflux until the completion of the reaction. Then the reaction mixture was acidified with 10 N HCl and the product was extracted with ethyl acetate, washed with water, dried over sodium sulfate, and concentrated. The product was purified by column chromatography on silica gel (hexane : ethyl acetate (4 : 1)) to afford the desired product.

Results and discussion

After the preparation of the catalyst, Fe_3O_4@SiO_2@SBA-3@2-ATP-Cu was extensively studied with several techniques such as XRD, SEM, atomic absorption, TGA, N_2 adsorption–desorption, and VSM. The XRD patterns of mesoporous silica (**1a**), Fe_3O_4@SiO_2@SBA-3@CPTMS (**1b**), Fe_3O_4@SiO_2@SBA-3@CPTMS@ATP (**1c**), and Fe_3O_4@SiO_2@SBA-3@2-ATP-Cu (**1d**) samples are shown in Fig. (1). The XRD patterns of arrayed silica nanoparticles show three diffraction peaks that can be indexed as the (111), (220), and (331) reflections that are arranged in a face-centered-cubic (fcc) structure (Fig. 1).[50] For all samples, peaks at 30.39°, 35.66°, 53.96°, 57.30°, and 62.94° correspond to the (220), (400), (422), (511), and (440) planes, which is in agreement with the literature (Fig. 1).[51] The XRD patterns of 2-aminothiophenol were not found in the XRD spectra.[52] The copper nanoparticles are responsible for the diffraction planes of

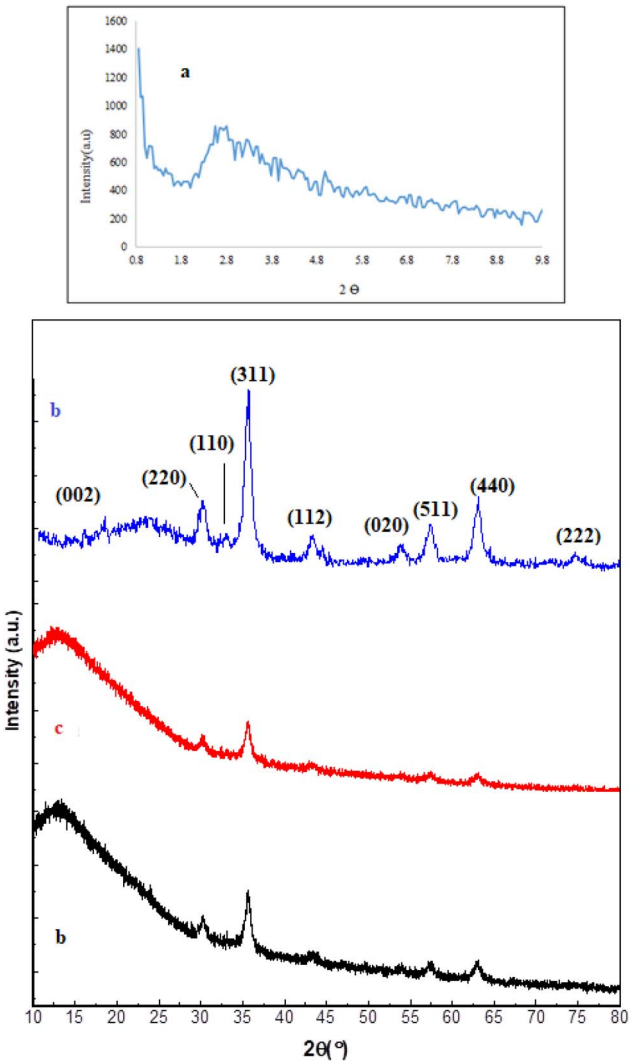

Fig. 1 XRD patterns of mesoporous silica (a), Fe_3O_4@SiO_2@SBA-3@CPTMS (b), Fe_3O_4@SiO_2@SBA-3@CPTMS@ATP (c), and Fe_3O_4@SiO_2@SBA-3@2-ATP-Cu (d).

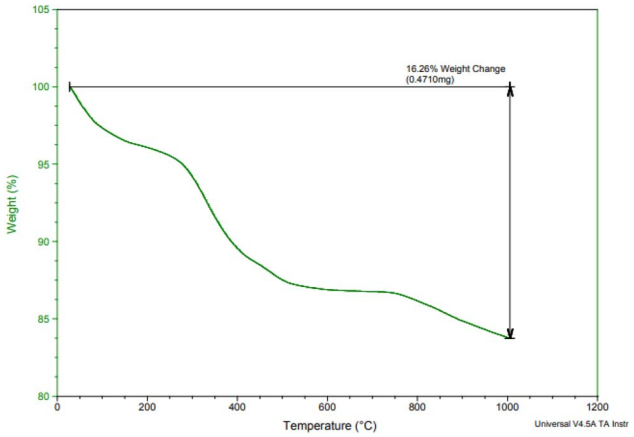

Fig. 2 TGA graph of Fe_3O_4@SiO_2@SBA-3@2-ATP-Cu.

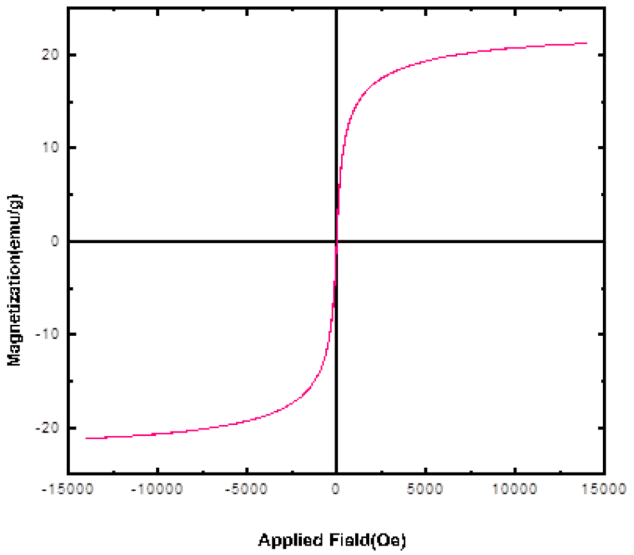

Fig. 3 Magnetization curves for Fe_3O_4@SiO_2@SBA-3@2-ATP-Cu at room temperature.

(002)[53] and the XRD pattern of Fe_3O_4@SiO_2@SBA-3@2-ATP-Cu, which showed the presence of characteristic peaks at 2θ values of 32, 42.3°, 55°, and 75°, related to (110), (112), (020), and (222) planes for both the conventional and green CuO, respectively.[54]

The Cu content of the prepared mesoporous magnetic material was determined by atomic absorption spectroscopy (AAS) and calculated to be 3.6×10^{-4} mol g^{-1}.

Fig. 2 displays the thermogravimetric analysis (TGA) of Fe_3O_4@SiO_2@SBA-3@2-ATP-Cu in the temperature range of 50–1000 °C. Results revealed a weight loss of about 8 wt% at a temperature of under 250 °C, which was related to the loss of water and the organic solvents. The maximum mass loss that occurred in the temperature range of 250 to 750 °C is due to the decomposition of immobilized organic moieties on the surface of magnetic mesoporous silica nanoparticles, and the amount of organic components was found to be about 10% of the total solid catalyst.

Fig. 3 shows the dependence of magnetization on the applied field (M–H) for Fe_3O_4@SiO_2@SBA-3@2-ATP-Cu at room temperature. The m*odified magnetic mesoporous* silica nanoparticle sample exhibited decreased magnetism due to the loading of 2-ATP-Cu on the surface of Fe_3O_4@SiO_2@SBA-3 compared to the bare Fe_3O_4@SiO_2@SBA-3.[48]

The size and structure of Fe_3O_4@SiO_2@SBA-3@2-ATP-Cu were evaluated using FE-SEM (Fig. 4). The results of the analysis showed uniformity and sphere-like morphology.

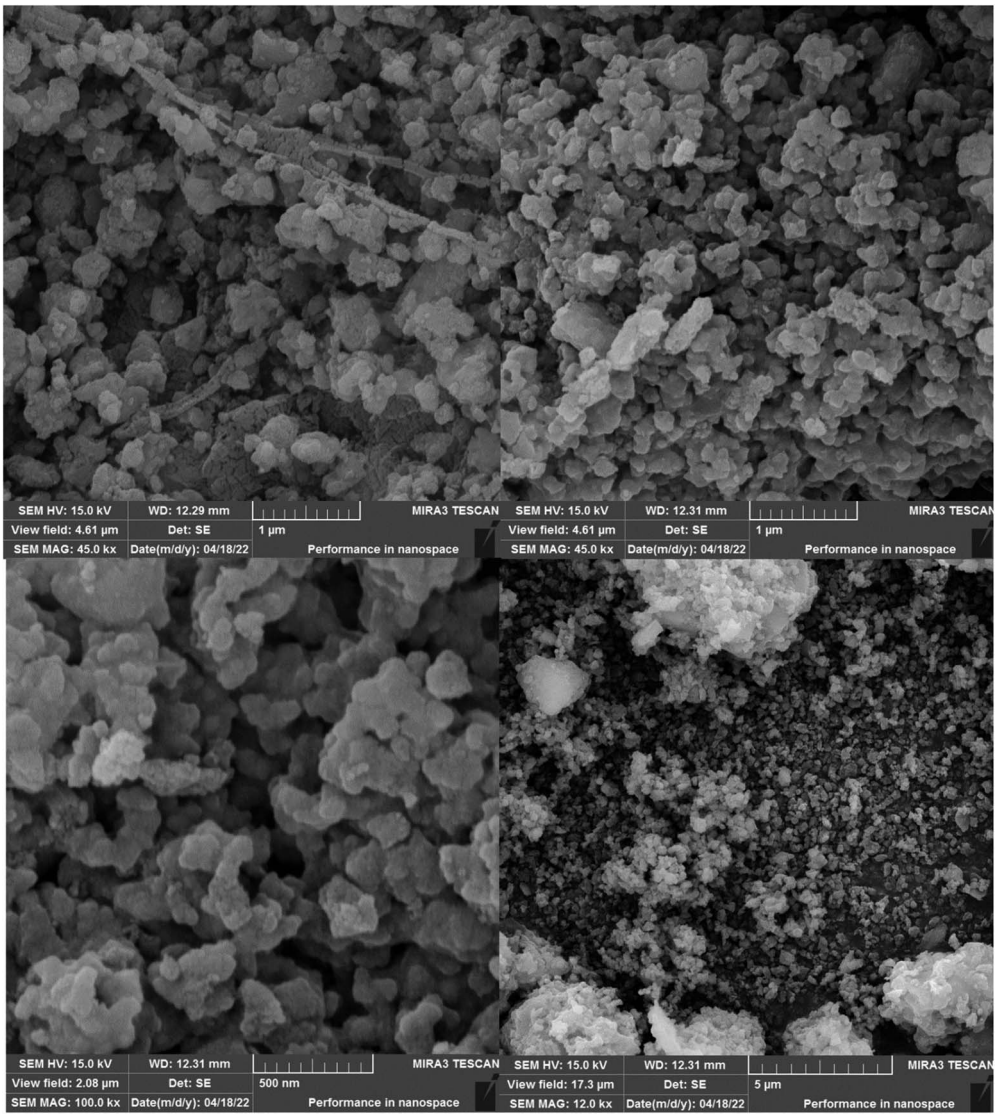

Fig. 4 SEM images of Fe_3O_4@SiO_2@SBA-3@2-ATP-Cu.

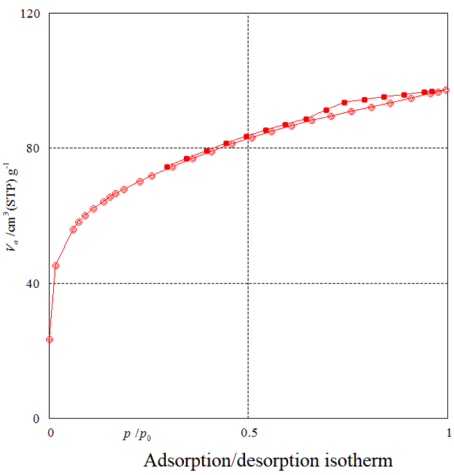

Fig. 5 N_2-adsorption isotherms of Fe_3O_4@SiO_2@SBA-3@2-ATP-Cu.

Nitrogen adsorption–desorption analysis gives us information on the mesoporous nature of Fe_3O_4@SiO_2@SBA-3@2-ATP-Cu. Fig. 5 shows a type II isotherm with an H3 type hysteresis loop in the range of 0.0–0.97 (P/P_0) for Fe_3O_4@SiO_2@SBA-3@2-ATP-Cu. The BET surface area of the prepared material was found to be 242 $m^2\ g^{-1}$. The textural data of the nanocatalysts are shown in Table 1. The

Table 1 Nitrogen adsorption–desorption data for Fe_3O_4@SiO_2@SBA-3@2-ATP-Cu

Entry	BET plot
V_m	55.72 $cm^3\ g^{-1}$
$a_{s,BET}$	242 $m^2\ g^{-1}$
Total pore volume ($p/p_0 = 0.990$)	0.15 $cm^3\ g^{-1}$
Mean pore diameter	2.48 nm

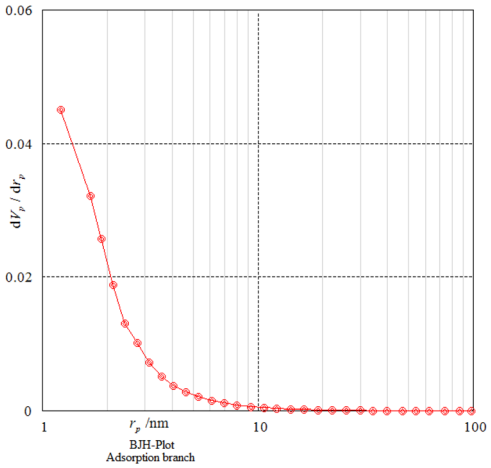

Fig. 6 BJH-plot of Fe_3O_4@SiO_2@SBA-3@2-ATP-Cu.

Table 2 BJH-plot data for Fe_3O_4@SiO_2@SBA-3@2-ATP-Cu

Plot data	Adsorption branch
V_p	0.0.07 cm^3 g^{-1}
r_p, peak(area)	1.22 nm
a_p	82.52 m^2g^{-1}

calculated mean pore diameter from the adsorption–desorption data using the BET procedure is 2.48 nm which further confirms the formation of the *mesoporous structure in the synthesized* material as shown in (Fig. 6, and Table 2).

Catalytic activity of Fe_3O_4@SiO_2@SBA-3@2-ATP-Cu for the synthesis of 5-substituted 1*H*-tetrazoles

To explore the catalytic activity of magnetic mesoporous silica nanoparticles, cycloaddition reactions of nitriles with sodium azide were investigated. Initially, the reaction of benzonitrile with sodium azide was selected as a model reaction to optimize the reaction conditions, such as various amounts of catalyst, solvents, and temperature (Table 3). First, the effect of solvents was studied and it was observed that the reaction was highly effective in PEG medium. Furthermore, the high efficiency of the reaction depended strongly on the amount of catalyst, which the reaction was completed in the presence of 60 mg of Fe_3O_4@SiO_2@SBA-3@2-ATP-Cu for 1 mmol of benzonitrile. The ideal temperature for the reaction was found to be 120 °C. Under these conditions, a wide range of benzonitrile derivatives were tolerated. This reaction proceeded well giving the desired products in high to excellent yields (Table 4).

Recyclability of the Fe_3O_4@SiO_2@SBA-3@2-ATP-Cu catalyst

The recovery of a catalyst is valuable and interesting from both the economic and the environmental aspects. To gain a better insight into the heterogeneity of Fe_3O_4@SiO_2@SBA-3@2-ATP-Cu, a catalytic reusability test was conducted using benzonitrile as a starting nitrile material. After each catalytic run, the catalyst was removed with an external magnet, washed, dried, and reused directly for the next run. Within four catalytic runs, the catalyst presented excellent reusability with no significant loss of the original catalytic yield (Fig. 7).

To show the accessibility of the present work, we summarize some of the results for the preparation of 5-substituted-1*H*-

Table 3 The optimization of reaction conditions[a]

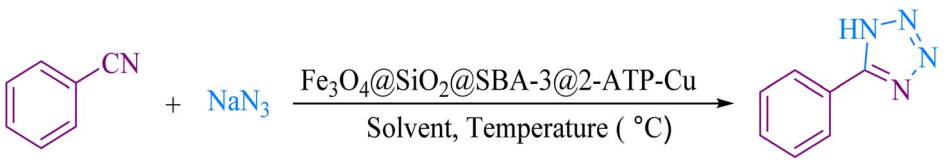

Entry	Solvent	Catalyst (mg)	Temperature (°C)	Time (min)	Yield[b] (%)
1	PEG	60	120	65	94
2	DMSO	60	120	65	78
3	DMF	60	120	65	82
4	H_2O	60	Reflux	65	N. R
5	PEG	50	120	65	81
6	PEG	40	120	65	73
7	PEG	60	100	65	77
8	PEG	60	80	65	48

[a] Reaction conditions: benzonitrile (1 mmol), sodium azide (1.1 mmol), catalyst, solvent (1 mL). [b] Isolated yield.

Table 4 Synthesis of 5-substituted-1*H*-tetrazoles in the presence of Fe_3O_4@SiO_2@SBA-3@2-ATP-Cu

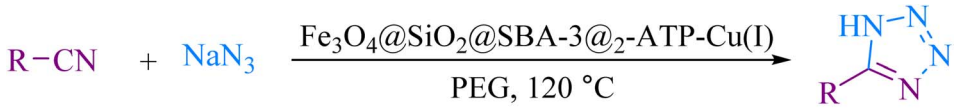

R : C_6H_5, 4-ClC_6H_4, 2-ClC_6H_4, 4-BrC_6H_4, 4-$NO_2C_6H_4$, 3-$NO_2C_6H_4$, 4-CNC_6H_4, 2-CNC_6H_4, 2-OHC_6H_4, 4-$COCH_3C_6H_4$, -$CH_2CO_2CH_3$, -$CH_2C_6H_6$, -$(CH_2)_3CH_3$, -CH_2CN

Entry[a]	Nitrile	Product	Time (min)	Yield[b] (%)	M.p. (°C) Found	M.p. (°C) Reported
1	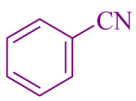	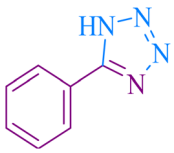	65	94	212–215	212–213 (ref. 55)
2	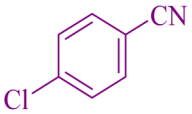	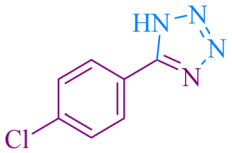	48	97	261–263	261–264 (ref. 55)
3	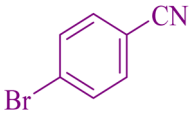	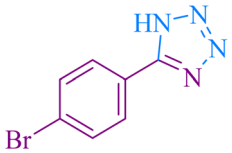	190	91	266–267	264–265 (ref. 56)
4	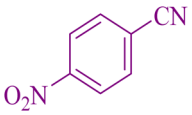	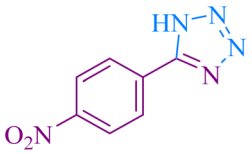	55	96	216–218	217–219 (ref. 55)
5	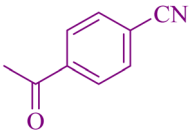	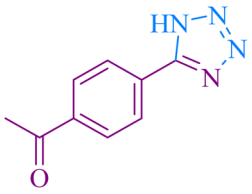	150	91	172–175	175–177 (ref. 57)
6	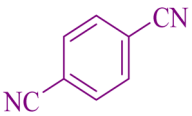	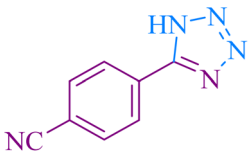	25	90	254–257	251–253 (ref. 55)
7	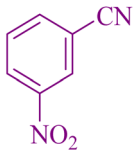	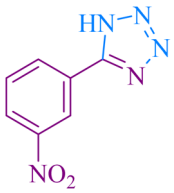	35	92	148–149	148–151 (ref. 55)

Table 4 (*Contd.*)

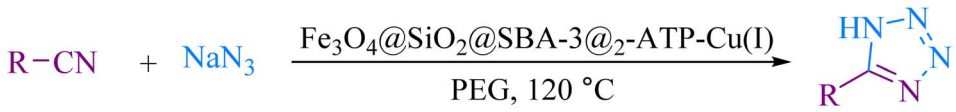

R : C_6H_5, 4-ClC_6H_4, 2-ClC_6H_4, 4-BrC_6H_4, 4-$NO_2C_6H_4$, 3-$NO_2C_6H_4$, 4-CNC_6H_4, 2-CNC_6H_4, 2-OHC_6H_4, 4-$COCH_3C_6H_4$, -$CH_2CO_2CH_3$, -$CH_2C_6H_6$, -$(CH_2)_3CH_3$, -CH_2CN

Entry[a]	Nitrile	Product	Time (min)	Yield[b] (%)	M.p. (°C) Found	M.p. (°C) Reported
8	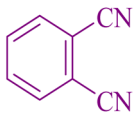	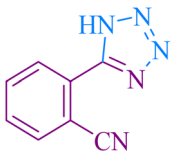	12	89	208–209	209–213 (ref. 58)
9	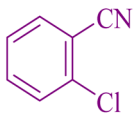		120	95	181–183	182–183 (ref. 55)
10	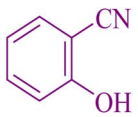	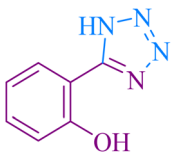	25	93	221–223	220–222 (ref. 58)
11	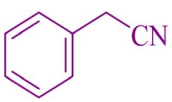	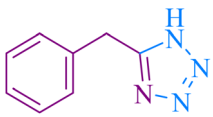	25	88	123–124	117–120 (ref. 56)

[a] Reaction conditions: nitrile (1 mmol), sodium azide (1.1 mmol), catalyst (60 mg), PEG (1 mL). [b] Isolated yield.

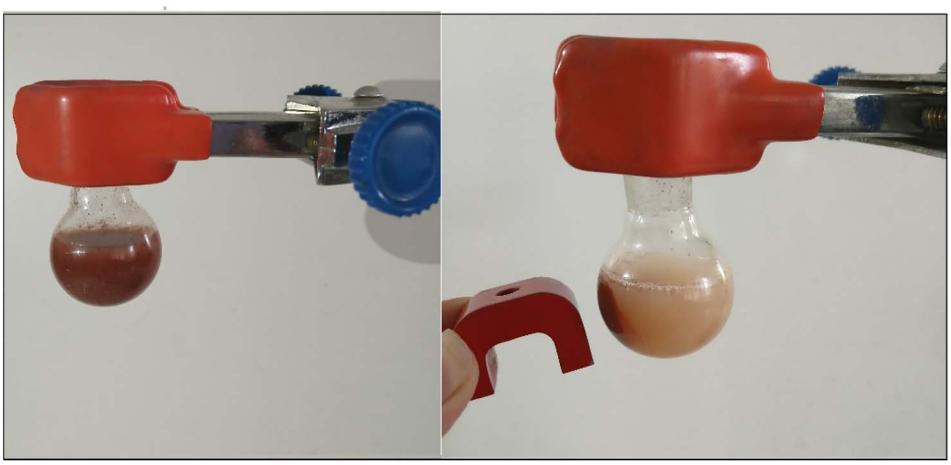

Fig. 7 Recyclability of Fe_3O_4@SiO_2@SBA-3@2-ATP-Cu.

Table 5 Comparison of the results for modified Fe_3O_4@SiO_2@SBA-3@2-ATP-Cu with other catalysts for the formation of 5-phenyl-1*H*-tetrazole

Entry	Catalyst	Conditions	Time (h)	Yield (%)	References
1	CuO/aluminosilicate	DMF, reflux	8	89	59
2	SiO_2-MTSA	DMF, 120 °C	6	83	60
3	Sm@l-MSN	DMF, 100 °C	5	94	61
4	Zn/Al hydrotalcite	DMF, 120 °C	12	84	62
5	Fe_3O_4@SiO_2@SBA-3@2-ATP-Cu	PEG, 120 °C	65 min	94	This work

tetrazoles in Table 5. The results show that modified *magnetic mesoporous* silica is the most efficient catalyst in terms of reaction time and yield.

Conclusion

In conclusion, Fe_3O_4@SiO_2@SBA-3@2-ATP-Cu was synthesized by a co-precipitation technique and exhibited efficient catalytic performance and outstanding recyclability for the synthesis of 5-substituted 1*H*-tetrazoles under relatively mild conditions. We hope the design and preparation of new magnetic mesoporous silica nanoparticles owing to their high surface area and thermal stability to be a step forward in the field of heterogenous catalysis development.

Data availability

All data generated or analyzed during this study are included in this published article [and its ESI† files].

Author contributions

Zahra Heidarnezhad: laboratory work, investigation, methodology. Arash Ghorbani-Choghamarani: resources, writing – review & editing, conceptualization, supervision. Zahra Taherinia: methodology, investigation, writing – original draft, validation.

Conflicts of interest

The authors declare that they have no known competing financial interests or personal relationships that could have appeared to influence the work reported in this paper.

Acknowledgements

The authors would like to thank the research facilities of Ilam University and Bu-Ali Sina University for financial support of this research project.

References

1 Z. A. Alothman, *Materials*, 2012, **5**, 2874–2902.
2 Y. Ma, W. Tong, H. Zhou and S. L. Suib, *Microporous Mesoporous Mater.*, 2000, **37**, 243–252.
3 W. L. Li, K. Lu and J. Y. Walz, *Int. Mater. Rev.*, 2012, **57**, 37–60.
4 K. Khanafer and K. Vafai, *Renewable Energy*, 2018, **123**, 398–406.
5 L. Zhu, D. Shen and K. H. Luo, *J. Hazard. Mater.*, 2020, **389**, 122102.
6 L. Ge, Y. Feng, Y. Dai, R. Wang and T. Ge, *Chem. Eng. J.*, 2023, **452**, 139116.
7 I. Mahboob, S. Shafique, I. Shafiq, P. Akhter, A. S. Belousov, P. L. Show, Y. K. Park and M. Hussain, *Environ. Res.*, 2023, **218**, 114983.
8 X. Xing, X. Ren, N. S. Alharbi and C. Chen, *J. Colloid Interface Sci.*, 2023, **629**, 744–754.
9 C. Rieg, M. Kirchhof, K. Gugeler, A. K. Beurer, L. Stein, K. Dirnberger, W. Frey, J. R. Bruckner, Y. Traa, J. Kästner, S. Ludwigs, S. Laschat and M. Dyballa, *Catal. Sci. Technol.*, 2022, **13**, 410–425.
10 R. Zaleski, M. Gorgol, J. Goworek, A. Kierys, M. Pietrow and B. Zgardzińska, *Adsorption*, 2019, **25**, 881–887.
11 B. Kilos, A. Tuel, M. Ziolek and J. C. Volta, *Catal. Today*, 2006, **118**, 416–424.
12 A. Galarneau, M. Nader, F. Guenneau, F. Di Renzo and A. Gedeon, *J. Phys. Chem. C*, 2007, **111**, 8268–8277.
13 K. kang Miao, X. lin Luo, W. Wang, J. le Guo, S. fan Guo, F. jiu Cao, Y. qiao Hu, P. mei Chang and G. dong Feng, *Microporous Mesoporous Mater.*, 2019, **289**, 109640.
14 H. Aghayan, A. R. Khanchi, T. Yousefi and H. Ghasemi, *J. Nucl. Mater.*, 2017, **496**, 207–214.
15 Y. Han, F. S. Xiao, S. Wu, Y. Sun, X. Meng, D. Li, S. Lin, F. Deng and X. Ai, *J. Phys. Chem. B*, 2001, **105**, 7963–7966.
16 J. Florek-Milewska, P. Decyk and M. Ziolek, *Appl. Catal., A*, 2011, **393**, 215–224.
17 A. Grünberg, X. Yeping, H. Breitzke and G. Buntkowsky, *Chem.–Eur. J.*, 2010, **16**, 6993–6998.
18 M. S. Khayoon and B. H. Hameed, *Appl. Catal., A*, 2013, **460–461**, 61–69.
19 E. Janiszewska, A. Held, K. Nowińska and S. Kowalak, *RSC Adv.*, 2019, **9**, 4671–4681.
20 E. Janiszewska, M. Zieliński, M. Kot, E. Kowalewski and A. Śrębowata, *ChemCatChem*, 2018, **10**, 4109–4118.
21 M. I. A. Abdel Maksoud, A. M. Elgarahy, C. Farrell, A. H. Al-Muhtaseb, D. W. Rooney and A. I. Osman, *Coord. Chem. Rev.*, 2020, **403**, 213096.
22 F. S. A. Khan, N. M. Mubarak, M. Khalid, R. Walvekar, E. C. Abdullah, S. A. Mazari, S. Nizamuddin and R. R. Karri, *Environ. Sci. Pollut. Res.*, 2020, **27**, 24342–24356.

23 S. A. H. Martínez, E. M. Melchor-Martínez, J. A. R. Hernández, R. Parra-Saldívar and H. M. N. Iqbal, *Fuel*, 2022, **312**, 122927.
24 S. Khizar, E. Elkalla, N. Zine, N. Jaffrezic-Renault, A. Errachid and A. Elaissari, *Expert Opin. Drug Deliv.*, 2023, **20**, 189–204.
25 Z. Hedayatnasab, A. Ramazani Saadatabadi, H. Shirgahi and M. R. Mozafari, *Mater. Res. Bull.*, 2023, **157**, 112035.
26 G. G. Flores-Rojas, F. López-Saucedo, R. Vera-Graziano, E. Mendizabal and E. Bucio, *Macromol*, 2022, **2**, 374–390.
27 K. Ghosal, S. Chatterjee, S. Thomas and P. Roy, *AAPS PharmSciTech*, 2023, **24**, 25.
28 Z. Li, W. Wan, Z. Bai, B. Peng, X. Wang, L. Cui, Z. Liu, K. Lin, J. Yang, J. Hao and F. Tian, *Sensor. Actuator. B Chem.*, 2023, **375**, 132869.
29 P. Amruth Maroju, R. Ganesan and J. Ray Dutta, *Mater. Today Proc.*, 2023, **72**, 62–66.
30 T. Lü, X. Zhang, R. Ma, D. Qi, Y. Sun, D. Zhang, J. Huang and H. Zhao, *Sep. Purif. Technol.*, 2023, **309**, 123097.
31 J. Zhang, S. Wang, Y. Ba and Z. Xu, *Eur. J. Med. Chem.*, 2019, **178**, 341–351.
32 A. Verma, B. Kaur, S. Venugopal, P. Wadhwa, S. Sahu, P. Kaur, D. Kumar and A. Sharma, *Chem. Biol. Drug Des.*, 2022, **100**, 419–442.
33 F. Gao, J. Xiao and G. Huang, *Eur. J. Med. Chem.*, 2019, **184**, 111744.
34 S. A. F. Rostom, H. M. A. Ashour, H. A. A. El Razik, A. E. F. H. A. El Fattah and N. N. El-Din, *Bioorganic Med. Chem.*, 2009, **17**, 2410–2422.
35 R. K. Uppadhayay, A. Kumar, J. Teotia and A. Singh, *Russ. J. Org. Chem.*, 2022, **58**, 1801–1811.
36 S. Bayomi, M. A. Moustafa, A. R. Maarouf and M. H. Aboutaleb, *J. Am. Sci.*, 2016, **12**, 40–56.
37 A. Ghorbani-Choghamarani and Z. Taherinia, *Aust. J. Chem.*, 2017, **70**, 1127–1137.
38 M. Nasrollahzadeh, Z. Nezafat, N. S. S. Bidgoli and N. Shafiei, *Mol. Catal.*, 2021, **513**, 111788.
39 A. H. Dabbagh and Y. Mansoori, *Dyes Pigm.*, 2002, **54**, 37–46.
40 M. Rösch, M. S. Gruhne, M. Lommel, S. M. J. Endraß and J. Stierstorfer, *Inorg. Chem.*, 2023, **62**, 1488–1507.
41 S. K. Prajapti, A. Nagarsenkar and B. N. Babu, *Tetrahedron Lett.*, 2014, **55**, 3507–3510.
42 P. Mani, A. K. Singh and S. K. Awasthi, *Tetrahedron Lett.*, 2014, **55**, 1879–1882.
43 S. Bhagat and V. Telvekar, *Synlett*, 2018, **29**, 874–879.
44 D. Amantini, R. Beleggia, F. Fringuelli, F. Pizzo and L. Vaccaro, *J. Org. Chem.*, 2004, **69**, 2896–2898.
45 F. Himo, Z. P. Demko, L. Noodleman and K. B. Sharpless, *J. Am. Chem. Soc.*, 2003, **125**, 9983–9987.
46 S. Kumar, S. Dubey, N. Saxena and S. K. Awasthi, *Tetrahedron Lett.*, 2014, **55**, 6034–6038.
47 B. Agrahari, S. Layek, R. Ganguly and D. D. Pathak, *New J. Chem.*, 2018, **42**, 13754–13762.
48 Z. Heidarnezhad, A. Ghorbani-Choghamarani and Z. Taherinia, *Catal. Lett.*, 2022, **152**, 3178–3191.
49 B. Tahmasbi and A. Ghorbani-Choghamarani, *New J. Chem.*, 2019, **43**, 14485–14501.
50 J. Wang, A. Sugawara-Narutaki, M. Fukao, T. Yokoi, A. Shimojima and T. Okubo, *ACS Appl. Mater. Interfaces*, 2011, **3**, 1538–1544.
51 A. Aashima, S. Uppal, A. Arora, S. Gautam, S. Singh, R. J. Choudhary and S. K. Mehta, *RSC Adv.*, 2019, **9**, 23129–23141.
52 T. E. Karpov, A. Rogova, D. R. Akhmetova, Y. A. Tishchenko, A. V. Chinakova, D. V. Lipin, N. V. Gavrilova, I. A. Gorbunova, S. A. Shipilovskikh and A. S. Timin, *Biomater. Sci.*, 2024, **12**, 3431–3445.
53 R. O. Aljedaani, S. A. Kosa and M. Abdel Salam, *Molecules*, 2022, **28**, 16.
54 G. Anbalagan, B. Subramanian, V. Suresh and P. Sivaperumal, *Cureus*, 2024, **16**(4), e57366.
55 M. A. Jani and K. Bahrami, *Appl. Organomet. Chem.*, 2020, **34**(12), e6014.
56 E. Aali, M. Gholizadeh and N. Noroozi-Shad, *J. Mol. Struct.*, 2022, **1247**, 131289.
57 P. Movaheditabar, M. Javaherian and V. Nobakht, *J. Iran. Chem. Soc.*, 2022, **19**, 1805–1816.
58 N. Moeini, M. Ghadermazi and S. Molaei, *J. Mol. Struct.*, 2022, **1251**, 131982.
59 P. Movaheditabar, M. Javaherian and V. Nobakht, *React. Kinet. Mech. Catal.*, 2017, **122**, 217–228.
60 D. H. Mahajan, D. Mistry and H. Tailor, *Chem. Sci.*, 2018, **7**(4), 676–686.
61 P. K. Samanta, R. Biswas, T. Das, M. Nandi, B. Adhikary, R. M. Richards and P. Biswas, *J. Porous Mater.*, 2019, **26**, 145–155.
62 M. L. Kantam, K. B. Shiva Kumar and K. Phani Raja, *J. Mol. Catal. A Chem.*, 2006, **247**, 186–188.